# Measurement of a Double Neutron-Spin Resonance and an Anisotropic Energy Gap for Underdoped Superconducting $NaFe_{0.985}Co_{0.015}As$ Using Inelastic Neutron Scattering

Chenglin Zhang,[1,2] Rong Yu,[1,3] Yixi Su,[4] Yu Song,[1,2] Miaoyin Wang,[2] Guotai Tan,[2,5] Takeshi Egami,[2,6,7] J. A. Fernandez-Baca,[7,2] Enrico Faulhaber,[8,9] Qimiao Si,[1] and Pengcheng Dai[1,2,*]

[1]*Department of Physics and Astronomy, Rice University, Houston, Texas 77005, USA*
[2]*Department of Physics and Astronomy, The University of Tennessee, Knoxville, Tennessee 37996-1200, USA*
[3]*Department of Physics, Renmin University of China, Beijing 100872, China*
[4]*Jülich Centre for Neutron Science, Forschungszentrum Jülich GmbH, Outstation at FRM II, Lichtenbergstrasse 1, D-85747 Garching, Germany*
[5]*Physics Department, Beijing Normal University, Beijing 100875, China*
[6]*Department of Materials Science and Engineering, The University of Tennessee, Knoxville, Tennessee 37996-1200, USA*
[7]*Oak Ridge National Laboratory, Oak Ridge, Tennessee 37831, USA*
[8]*Gemeinsame Forschergruppe HZB - TU Dresden, Helmholtz-Zentrum Berlin für Materialien und Energie, D-14109 Berlin, Germany*
[9]*Forschungsneutronenquelle Heinz Maier-Leibnitz (FRM-II), TU München, D-85747 Garching, Germany*

(Received 22 June 2013; published 12 November 2013)

We use inelastic neutron scattering to show that superconductivity in electron-underdoped $NaFe_{0.985}Co_{0.015}As$ induces a dispersive sharp resonance near $E_{r1} = 3.25$ meV and a broad dispersionless mode at $E_{r2} = 6$ meV. However, similar measurements on overdoped superconducting $NaFe_{0.935}Co_{0.045}As$ find only a single sharp resonance at $E_r = 7$ meV. We connect these results with the observations of angle-resolved photoemission spectroscopy that the superconducting gaps in the electron Fermi pockets are anisotropic in the underdoped material but become isotropic in the overdoped case. Our analysis indicates that both the double neutron spin resonances and gap anisotropy originate from the orbital dependence of the superconducting pairing in the iron pnictides. Our discovery also shows the importance of the inelastic neutron scattering in detecting the multiorbital superconducting gap structures of iron pnictides.

DOI: 10.1103/PhysRevLett.111.207002 PACS numbers: 74.25.Ha, 74.25.Jb, 74.70.−b, 78.70.Nx

High-transition temperature (high-$T_c$) superconductivity in copper oxides and iron pnictdies can be derived from electron or hole doping to their antiferromagnetic (AFM) parent compounds [1,2]. Since magnetism may underlie the electron pairing in high-$T_c$ superconductors [3], it is important to determine how magnetic excitations can probe the superconducting (SC) electron pairing interactions. For single band copper oxide superconductors, the neutron spin resonance, a sharp collective magnetic excitation at the AFM ordering wave vector below $T_c$, has been the subject of twenty years' study and provided strong evidence for the sign changing nature of the $d$-wave superconducting gap in these materials [4]. In the case of multiband iron pnictide superconductors [5,6], band structure calculations indicate that the Fermi surfaces consist of hole pockets near the zone center and electron pockets near the zone corner [7–11]. Although the sign change of the quasiparticle excitations (nesting) between the hole and electron pockets also necessitates a resonance at an energy below the sum of the electron and hole SC gap energies [12,13], the multiple $3d$ Fe orbital nature of the iron pnictides [14,15] means that the SC gaps can be anisotropic on different Fermi surfaces [16,17]. Therefore, if the resonance is a direct probe of the quasiparticle excitations between the hole and electron Fermi pockets, it should be sensitive to the SC gap energy anisotropy. In spite of intensive inelastic neutron scattering (INS) work on the hole [18–20] and electron-doped [21–24] $BaFe_2As_2$ family of iron pnictides, only a broad resonance consistent with the sign change of the SC pairing has been observed.

For the $NaFe_{1-x}Co_xAs$ family of iron pnictides [Fig. 1(a)] [25,26], the London penetration depth measurements suggest that the SC gap is highly anisotropic even at optimal doping [27]. Moreover, angle-resolved photoemission (ARPES) experiments indicate the presence of a large SC gap anisotropy in the electron Fermi pockets of the underdoped regime near $x = 0.0175$, which is absent in the hole Fermi pockets; the gap anisotropy disappears upon increasing $x$ to 0.045 [Figs. 1(c) and 1(d)] [28–30]. A likely origin [31] of this gap anisotropy is the angular variation of the relative orbital weight among the $d_{xy}$ and the degenerate $d_{xz/yz}$ orbitals along the electron Fermi pockets, which is absent along the hole Fermi pockets. As such, this material offers the opportunity to study the role of orbital dependence in SC pairing via INS.

In this Letter, we present an INS study of spin excitations in underdoped SC $NaFe_{0.985}Co_{0.015}As$ coexisting with static AFM order ($T_c = 15$ K, $T_N = 30$ K) and its comparison with overdoped SC $NaFe_{0.935}Co_{0.045}As$ ($T_c = 18$ K) [Fig. 1(a)] [32]. Our INS experiments reveal that superconductivity induces two distinct neutron spin resonances at the commensurate AFM wave vector $\mathbf{Q} = (0.5, 0.5, L)$ in

 

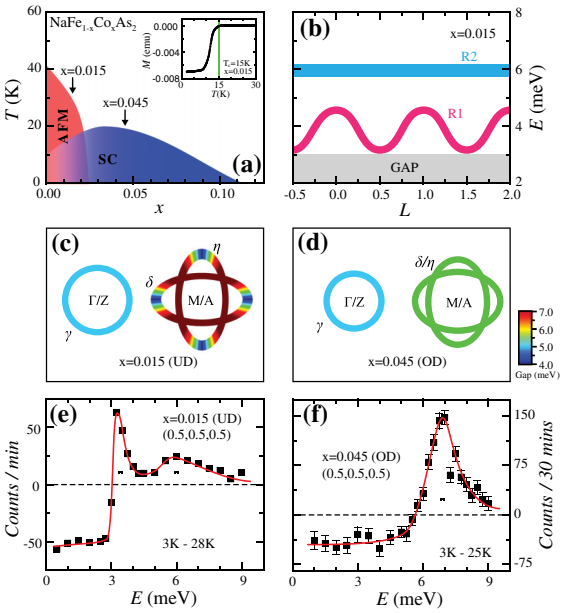


FIG. 1 (color online). (a) The electronic phase diagram of $NaFe_{1-x}Co_xAs$, where the arrows indicate the Co-doping levels of our samples. The temperature dependence of the bulk susceptibility in the inset shows $T_c = 15$ K. (b) The schematics of the $c$-axis dispersion of the double resonances. (c), (d) The schematics of Fermi surfaces and SC gaps in underdoped and overdoped samples near Γ and $M$ points [28]. (e) Double resonances obtained by taking temperature difference plots (3 K–28 K) of constant-$Q$ scans at (0.5, 0.5, 0.5) in $NaFe_{0.985}Co_{0.015}As$. (f) Similar data in $NaFe_{0.935}Co_{0.045}As$ showing only a single resonance. The horizontal bars in (e) and (f) indicate instrumental energy resolution.

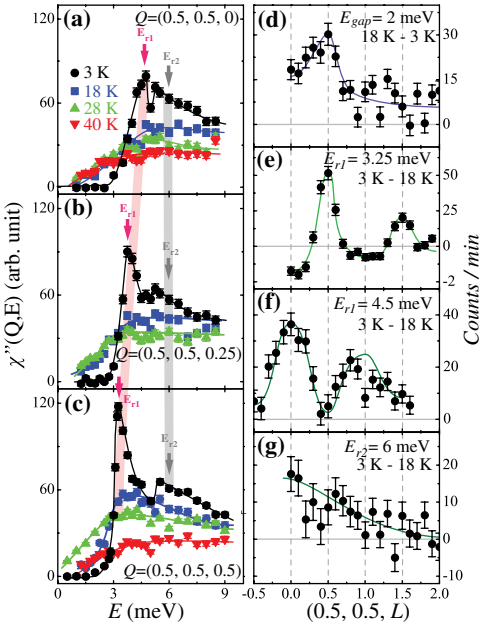


FIG. 2 (color online). (a)–(c) $\chi''(Q, E)$ at $\mathbf{Q} = (0.5, 0.5, L)$ with $L = 0$, 0.25 and 0.5, respectively, at 3, 18, 28 and 40 K. (d)–(g) The difference of $L$-modulations above and below $T_c$ at $E = 2$, 3.25, 4.5 and 6 meV, respectively.

$NaFe_{0.985}Co_{0.015}As$ [Figs. 2(a)–2(c)]; this is an entirely new behavior which has never been observed in either the iron-based or copper-based superconductors. While the first resonance occurring at $E_{r1} = 3.25$ meV is sharp in energy and becomes dispersive along the $c$ axis, there is also a broad dispersionless resonance at $E_{r2} = 6$ meV [Figs. 2(e)–2(g)]. For electron-overdoped SC $NaFe_{0.935}Co_{0.045}As$, the double resonances change back to a single resonance [Fig. 1(f)] [32]. Our analysis indicates that both the SC gap anisotropy and the double resonances arise from the orbital dependent pairing strength, and reveals the important role that INS can play in probing of the multiorbital structure of superconductivity in the iron-based superconductors.

We prepared ~5 g single crystals of $NaFe_{0.985}Co_{0.015}As$ by the self-flux method. Susceptibility [inset in Fig. 1(a)], heat capacity [33], and nuclear magnetic resonance [34] measurements showed that the sample is a homogeneous bulk superconductor ($T_c = 15$ K) microscopically coexisting with static AFM order. Our neutron scattering experiments were carried out on the thermal (HB-3) and cold (PANDA) triple-axis spectrometers at the High Flux Isotope Reactor, Oak Ridge National Laboratory and the FRM-II, TU Müchen, Germany [22], respectively. At HB-3, we fixed final neutron energies at $E_f = 14.7$ meV with a pyrolytic graphite (PG) monochromator and analyzer. At PANDA, We used a focusing PG monochromator and analyzer with a fixed final neutron energy of $E_f = 5$ meV. The wave vector $\mathbf{Q}$ at ($q_x$, $q_y$, $q_z$) in Å$^{-1}$ is defined as $(H, K, L) = (q_x a/2\pi, q_y a/2\pi, q_z c/2\pi)$ reciprocal lattice unit (rlu) using the tetragonal unit cell (space group $P4/nmm$, $a \approx 3.952$ Å and $c = 6.980$ Å at 3 K). In this notation, the AFM Bragg peaks occur at the (0.5, 0.5, $L$) positions with $L = 0.5, 1.5, \ldots$ [25]. The samples are coaligned in the [$H$, $H$, $L$] scattering zones with a mosaic less than 2°. Figure 4(a) shows the temperature dependence of the elastic scattering at $\mathbf{Q}_{\mathrm{AFM}} = (0.5, 0.5, 0.5)$, which reveals a clear reduction at the onset of $T_c$ and dramatic increase below $T_N = 30$ K [Fig. 4(a)]. These results suggest that $NaFe_{0.985}Co_{0.015}As$ is a homogeneous electron underdoped superconductor similar to underdoped SC $BaFe_{2-x}T_xAs_2$ ($T$ = Co, Ni) [Fig. 1(a)] [35,36]. From earlier ARPES measurements [28–30], we know that the SC gaps in the electron and hole pockets are quite isotropic for electron overdoped $NaFe_{0.935}Co_{0.045}As$ [Fig. 1(d)], but the SC gap becomes highly anisotropic for $NaFe_{0.985}Co_{0.015}As$ [Fig. 1(c)].

In previous INS work on overdoped $NaFe_{0.935}Co_{0.045}As$, a dispersionless sharp resonance was found at $E_r = 7$ meV below $T_c$ [Fig. 1(f)] [32]. To explore what happens in the underdoped regime where superconductivity coexists with AFM static order [34], we carried out constant-$\mathbf{Q}$ scans at wave vectors $\mathbf{Q} = (0.5, 0.5, L)$ with $L = 0$, 0.25, and 0.5 rlu at $T < T_c$, $T_c < T < T_N$, and $T > T_N$ on $NaFe_{0.985}Co_{0.015}As$. Figures 2(a)–2(c) show the $\chi''(Q, E)$ at $T = 3$, 18, 28, 40 K, obtained by subtracting the background scattering of $\mathbf{Q}$ scans in Fig. 3 and correcting for the Bose population

factor using $\chi''(Q,E)=[1-\exp(-E/k_BT)]S(Q,E)$, where $S(Q, E)$ is the magnetic scattering function. At $T = 40$ K ($T = T_N + 10$ K), the paramagnetic scattering at all three wave vectors probed are relaxational and can be fitted with $\chi''(Q, E) \propto E/(\Gamma^2 + E^2)$ as shown in solid lines in Figs. 2(a)–2(c). On cooling to $T = 28$ K ($T = T_N - 2$ K), the overall line shape of the scattering remain unchanged. On further cooling to $T = 18$ K ($T = T_c + 3$ K), while the scattering at wave vectors $\mathbf{Q} = (0.5, 0.5, L)$ with $L = 0$, 0.25 still have Lorentzian line shape (relaxational) [blue symbols in Figs. 2(a) and 2(b)], a spin anisotropy gap of $\sim$1.5 meV opens at $\mathbf{Q}_{\mathrm{AFM}} = (0.5, 0.5, 0.5)$ [blue symbols in Fig. 2(c)]. Finally, upon entering into the SC state at $T = 3$ K ($T = T_c - 12$ K), we see that a sharp resonance and a broad resonance develop at $E_{r1}=3.25$ and $E_{r2} = 6$ meV, respectively, at $\mathbf{Q}_{\mathrm{AFM}} = (0.5, 0.5, 0.5)$ [Fig. 2(c)]. In addition, the normal state spin gap of $\sim$1.5 meV increases to $\sim$3 meV below $T_c$ [Fig. 2(c)]. The temperature difference plot between 3 and 28 K shown in Fig. 1(e) confirms the presence of superconductivity-induced double resonances. On changing wave vectors to $\mathbf{Q} = (0.5, 0.5, 0.25)$ and $\mathbf{Q} = (0.5, 0.5, 0)$, we see a clear increase in energy of the sharp resonance while the broad mode remains at $E_{r2} = 6$ meV [Figs. 2(a) and 2(b)]. However, the low-temperature spin gaps are similar at all wave vectors.

To probe the $c$-axis modulations of the low-energy spin excitations and superconductivity-induced effect, we carried out constant-energy scans along the [0.5, 0.5, $L$] direction at different energies above and below $T_c$. Since there is a low-temperature spin gap below $\sim$3 meV, the $L$ dependence of the normal state magnetic scattering at $E = 2$ meV can be obtained by subtracting the data at $T = 3$ K from those at 18 K. The magnetic scattering at $E = 2$ meV and 18 K shows a broad peak at $\mathbf{Q}_{\mathrm{AFM}}$ with $L = 0.5$ rlu [Fig. 2(d)]. At the first resonance energy ($E_{r1} = 3.25$ meV), superconductivity induces well-defined peaks centered at $\mathbf{Q}_{\mathrm{AFM}} = [0.5, 0.5, L]$ with $L = 0.5$, 1.5 [Fig. 2(e)]. The energy of the first resonance moves to $E_{r1} = 4.5$ meV at [0.5, 0.5, $L$] with $L = 0$, 1, as illustrated in Fig. 2(f). Figure 2(g) shows that the second resonance at $E_r = 6$ meV is indeed dispersionless with superconductivity-induced enhancement below $T_c$ decreases monotonically with increasing $L$, following the Fe magnetic form factor.

To confirm the low-temperature spin gap and determine the wave vector dependence of the resonances, we carried out constant-energy scans at different energies above and below $T_c$, and above $T_N$. Figures 3(a)–3(f) show $S(Q, E)$ along the [$H$, $H$, 0] and [$H$, $H$, 0.5] directions, respectively. At $E = 2$ meV, a well-defined Gaussian peak in the normal state disappears below $T_c$, confirming the presence of the low-temperature spin gap [Figs. 3(a) and 3(d)]. Comparing $E_{r1} = 4.5$ meV with $L = 0$ [Fig. 3(b)] and $E_{r1} = 3.25$ meV with $L = 0.5$ [Fig. 3(e)], we see that the intensity gain of the resonances below $T_c$ is larger at $L = 0.5$. At the second resonance energy $E_{r2} = 6$ meV [Figs. 3(e) and 3(f)], superconductivity-induced intensity

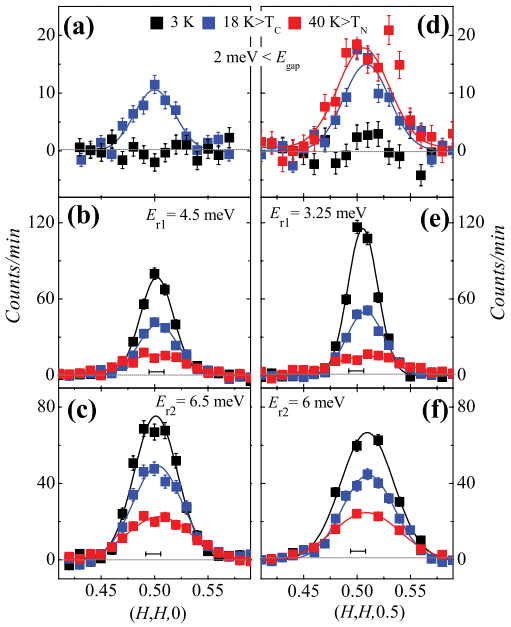


FIG. 3 (color online). (a)–(c) $\mathbf{Q}$ scans along the [$H$, $H$, 0] direction at $E = 2$ meV, $E_{r1} = 4.5$ meV, and $E_{r2} = 6.5$ meV, respectively, with $L = 0$. (d)–(f) $\mathbf{Q}$ scans along the [$H$, $H$, 0.5] direction at $E = 2$ meV, $E_{r1} = 3.25$ meV, and $E_{r2} = 6$ meV, respectively, for SC $NaFe_{0.985}Co_{0.015}As$. The horizontal bars indicate instrumental resolution. The solid lines are fits to Gaussians.

gain decreases with increasing $L$. By Fourier transforming the fitted Guassian peaks, we find that the spin-spin correlation lengths above $T_N$ are $\xi = 33 \pm 2$ Å at $L = 0$, 0.5. At 3 K and $L = 0$, spin correlation lengths increase to $\xi = 67 \pm 2$ and $52 \pm 2$ Å at $E_{r1} = 4.5$ and $E_{r2} = 6.5$ meV, respectively. At 3 K and $L = 0.5$, they are $75 \pm 2$ and $42 \pm 2$ Å at 3.25 and 6 meV, respectively.

Figures 4(a)–4(f) summarize the temperature dependence of the scattering at different energies and wave vectors. At the elastic AFM Bragg position, we see a clear effect of $T_N$ and $T_c$ [Fig. 4(a)]. For $E = 2$ meV, spin excitations show a kink at $T_N$ signaling the static AFM order, and decrease on cooling below $T_c$ [Figs. 4(b) and 4(c)]. From Figs. 4(d) and 4(f), we see that while the intensity at resonance energies show kinks at $T_N$, they increase dramatically below $T_c$. These results provide conclusive evidence of the presence of double resonance in underdoped $NaFe_{0.985}Co_{0.015}As$.

In iron pnictides, the Fermi surface is composed of multiple orbitals. In electron doped $NaFe_{1-x}Co_xAs$, the dominant orbital character of the electron pockets would be either $d_{xy}$ or $d_{xz/yz}$, depending on the direction in the Brillouin zone [Figs. 1(c) and 1(d)] [28–30]. Recent theories and experiments find that the effective strength of electron correlations can be very different between the $d_{xy}$ and $d_{xz/yz}$ orbitals [15,37–39]. This may induce orbital-selective SC pairing strengths, which naturally give anisotropic SC gaps along the electron pockets. The neutron resonance in the SC state is a bound state at energies just below the particle-hole excitation energy $E_r \leq \Delta_h + \Delta_e$

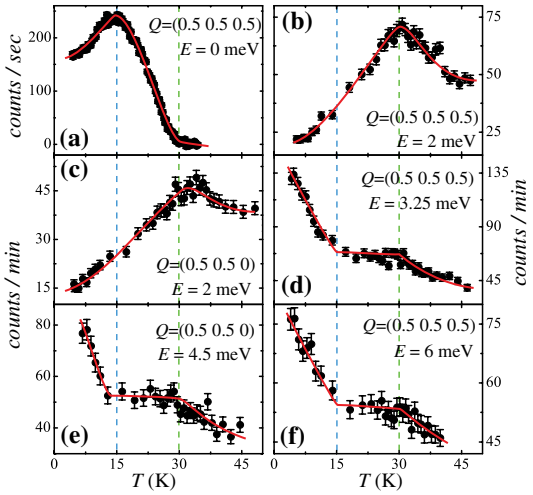


FIG. 4 (color online). (a) The temperature dependence of AFM peak intensity at $\mathbf{Q} = (0.5, 0.5, 0.5)$ with vertical dashed line indicating $T_c = 15$ K and $T_N = 30$ K. (b) and (c) Temperature dependence of the scattering at $E = 2$ meV at $\mathbf{Q} = (0.5, 0.5, 0)$ and (0.5, 0.5, 0.5), respectively. Temperature dependence of the scattering at (d) $E_{r1} = 3.25$ meV and (0.5, 0.5, 0.5), (e) $E_{r2} = 4.5$ meV and (0.5, 0.5, 0), and (f) $E_{r2} = 6$ meV and (0.5, 0.5, 0.5).

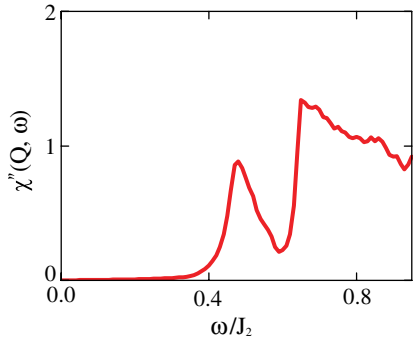


FIG. 5 (color online). The imaginary part of the dynamical susceptibility, $\chi''(\mathbf{Q}, \omega)$ at $\mathbf{Q} = (\pi, 0)$ in the SC phase obtained from a five-orbital t-$J_1$-$J_2$ model. For the case of sufficiently large gap anisotropy shown here, two resonance peaks are obtained.

[4]. If the anisotropic SC gap in the electron pocket is large, as in the underdoped $NaFe_{0.985}Co_{0.015}As$, there are two characteristic gaps $\Delta_{e1} \neq \Delta_{e2}$ (respectively associated with $d_{xy}$ and $d_{xz/yz}$ orbitals). Two resonance peaks are expected as a result of this separation of energy scales. As the electron doping is increased to the overdoped regime, the orbital selectivity of the correlations is reduced [39], which would give rise to a smaller SC gap anisotropy with $\Delta_{e1} \approx \Delta_{e2}$. Therefore, only one resonance peak would be resolved.

The above picture [31] is supported by our theoretical calculation of the dynamical spin susceptibility in the SC state of a multiorbital $t - J_1 - J_2$ model [17,40]. The Hamiltonian reads $H = H_0 + H_{\text{int}}$. Here, $H_0$ contains a five-orbital tight-binding model adapted from Ref. [41]. We have modified some tight-binding parameters such that the band structure better fits to the density functional theory results on NaFeAs. The interaction part $H_{\text{int}}$ includes matrix $J_1 - J_2$ couplings. Figure 5 shows the calculated imaginary part of the dynamic susceptibility, $\chi''(\mathbf{Q}, \omega)$ where $E = \hbar\omega$. Indeed we find two resonance peaks when the gap anisotropy is large, which turn into one sharp peak when the gap anisotropy is reduced.

We now turn to several remarks. First, in the underdoped regime where the SC and AFM states coexist, a reconstruction of the Fermi surface in the AFM state may in principle cause a SC gap anisotropy. However, this mechanism is unlikely because ARPES observes neither the Fermi surface reconstruction nor any gap anisotropy on the hole Fermi pocket in the underdoped $NaFe_{1-x}Co_xAs$ [28]. Second, one may in principle consider the double spin resonances as originating from the quasiparticle excitations between two different hole and electron Fermi pockets with different SC gaps. However, such an effect would lead to spin resonances at different wave vectors due to mismatched Fermi surfaces [42]. This is unlike our observation here that both resonances appear at the same commensurate wave vector. Third, we have emphasized the orbital selectivity in understanding the data. Through a spin-orbit coupling, this orbital-dependent effect may also lead to a spin anisotropy in the fluctuation spectrum.

In conclusion, we use INS to find two resonances at the same commensurate AFM wave vector for the underdoped $NaFe_{0.985}Co_{0.015}As$, but only one resonance for the overdoped SC $NaFe_{0.935}Co_{0.045}As$. This is different from the $c$-axis dispersion of the resonance in electron-doped $BaFe_{1.9}Ni_{0.1}As_2$ [22] and hole-doped copper oxide superconductor $YBa_2Cu_3O_{6.85}$ [43]. The doping evolution of the spin resonance coincides with that of the SC gap anisotropy in ARPES experiments. Our experimental discoveries, together with our theoretical analysis, suggest that both properties arise from the orbital dependence of the SC pairing. This provides evidence that the orbital selectivity plays an important role in understanding the SC pairing of the multiorbital electrons in the iron pnictides. Because the multiplicity of electron orbitals is a distinct feature of the iron-based superconductors and likely makes a major contribution to their superconducting pairing, our results will be important to the eventual understanding of superconductivity in these and related materials.

We thank C. Redding and Scott Carr for their help in the sample making process. The work at Rice/UTK was supported by the U.S. DOE, BES, through Contract No. DE-FG02-05ER46202 (P. D.). Work at Rice University was supported by the NSF Grant No. DMR-1309531 and the Robert A. Welch Foundation Grant No. C-1411 (Q. S.). C. L. Z. and T. E. are partially supported by the U.S. DOE BES through the EPSCoR Grant No. DE-FG02-08ER46528. The work at the High Flux Isotope Reactor was partially supported by the Division of Scientific User Facilities, U.S. DOE, BES. R. Y. is partially supported by NSFC Grant No. 11374361.

*pdai@rice.edu


[1] J. M. Tranquada, G. Xu, and I. A. Zaliznyak, J. Magn. Magn. Mater. **350**, 148 (2014).
[2] P. C. Dai, J. P. Hu, and E. Dagotto, Nat. Phys. **8**, 709 (2012).
[3] D. J. Scalapino, Rev. Mod. Phys. **84**, 1383 (2012).
[4] M. Eschrig, Adv. Phys. **55**, 47 (2006).
[5] Y. Kamihara, T. Watanabe, M. Hirano, and H. Hosono, J. Am. Chem. Soc. **130**, 3296 (2008).
[6] C. W. Chu, F. Chen, M. Gooch, A. M. Guloy, B. Lorenz, B. Lv, K. Sasmal, Z. J. Tang, J. H. Tapp, and Y. Y. Xue, Physica (Amsterdam) **469C**, 326 (2009).
[7] D. J. Singh and M. H. Du, Phys. Rev. Lett. **100**, 237003 (2008).
[8] K. Kuroki, S. Onari, R. Arita, H. Usui, Y. Tanaka, H. Kontani, and H. Aoki, Phys. Rev. Lett. **101**, 087004 (2008).
[9] I. I. Mazin, D. J. Singh, M. D. Johannes, and M. H. Du, Phys. Rev. Lett. **101**, 057003 (2008).
[10] P. J. Hirschfeld, M. M. Korshunov, and I. I. Mazin, Rep. Prog. Phys. **74**, 124508 (2011).
[11] A. Chubukov, Annu. Rev. Condens. Matter Phys. **3**, 57 (2012).
[12] M. M. Korshunov and I. Eremin, Phys. Rev. B **78**, 140509 (R) (2008).
[13] T. A. Maier, S. Graser, D. J. Scalapino, and P. Hirschfeld, Phys. Rev. B **79**, 134520 (2009).
[14] M. Yi, D. H. Lu, J. G. Analytis, J.-H. Chu, S.-K. Mo, R.-H. He, R. G. Moore, X. J. Zhou, G. F. Chen, J. L. Luo, N. L. Wang, Z. Hussain, D. J. Singh, I. R. Fisher, and Z.-X. Shen, Phys. Rev. B **80**, 024515 (2009).
[15] M. Yi, D. H. Lu, R. Yu, S. C. Riggs, J.-H. Chu, B. Lv, Z. K. Liu, M. Lu, Y.-T. Cui, M. Hashimoto, S.-K. Mo, Z. Hussain, C. W. Chu, I. R. Fisher, Q. Si, and Z.-X. Shen, Phys. Rev. Lett. **110**, 067003 (2013).
[16] T. A. Maier, S. Graser, D. J. Scalapino, and P. J. Hirschfeld, Phys. Rev. B **79**, 224510 (2009).
[17] P. Goswami, P. Nikolic, and Q. Si, Europhys. Lett. **91**, 37006 (2010).
[18] A. D. Christianson, E. A. Goremychkin, R. Osborn, S. Rosenkranz, M. D. Lumsden, C. D. Malliakas, I. S. Todorov, H. Claus, D. Y. Chung, M. G. Kanatzidis, R. I. Bewley, and T. Guidi, Nature (London) **456**, 930 (2008).
[19] C. L. Zhang, M. Wang, H. Q. Luo, M. Y. Wang, M. S. Liu, J. Zhao, D. L. Abernathy, T. A. Maier, K. Marty, M. D. Lumsden, S. Chi, S. Chang, J. A. Rodriguez-Rivera, J. W. Lynn, T. Xiang, J. P. Hu, and P. C. Dai, Sci. Rep. **1**, 115 (2011).
[20] J.-P. Castellan, S. Rosenkranz, E. A. Goremychkin, D. Y. Chung, I. S. Todorov, M. G. Kanatzidis, I. Eremin, J. Knolle, A. V. Chubukov, S. Maiti, M. R. Norman, F. Weber, H. Claus, T. Guidi, R. I. Bewley, and R. Osborn, Phys. Rev. Lett. **107**, 177003 (2011).
[21] M. D. Lumsden, A. D. Christianson, D. Parshall, M. B. Stone, S. E. Nagler, G. J. MacDougall, H. A. Mook, K. Lokshin, T. Egami, D. L. Abernathy, E. A. Goremychkin, R. Osborn, M. A. McGuire, A. S. Sefat, R. Jin, B. C. Sales, and D. Mandrus, Phys. Rev. Lett. **102**, 107005 (2009).
[22] S. Chi, A. Schneidewind, J. Zhao, L. W. Harriger, L. J. Li, Y. K. Luo, G. H. Cao, Z. A. Xu, M. Loewenhaupt, J. P. Hu, and P. C. Dai, Phys. Rev. Lett. **102**, 107006 (2009).
[23] D. S. Inosov, J. T. Park, P. Bourges, D. L. Sun, Y. Sidis, A. Schneidewind, K. Hradil, D. Haug, C. T. Lin, B. Keimer, and V. Hinkov, Nat. Phys. **6**, 178 (2010).
[24] P. Steffens, C. H. Lee, N. Qureshi, K. Kihou, A. Iyo, H. Eisaki, and M. Braden, Phys. Rev. Lett. **110**, 137001 (2013).
[25] S. L. Li, C. de la Cruz, Q. Huang, G. F. Chen, T.-L. Xia, J. L. Luo, N. L. Wang, and P. C. Dai, Phys. Rev. B **80**, 020504(R) (2009).
[26] D. R. Parker, M. J. P. Smith, T. Lancaster, A. J. Steele, I. Franke, P. J. Baker, F. L. Pratt, M. J. Pitcher, S. J. Blundell, and S. J. Clarke, Phys. Rev. Lett. **104**, 057007 (2010).
[27] K. Cho, M. A. Tanatar, N. Spyrison, H. Kim, Y. Song, P. C. Dai, C. L. Zhang, and R. Prozorov, Phys. Rev. B **86**, 020508(R) (2012).
[28] Q. Q. Ge, Z. R. Ye, M. Xu, Y. Zhang, J. Jiang, B. P. Xie, Y. Song, C. L. Zhang, P. C. Dai, and D. L. Feng, Phys. Rev. X **3**, 011020 (2013).
[29] Z.-H. Liu, P. Richard, K. Nakayama, G.-F. Chen, S. Dong, J.-B. He, D.-M. Wang, T.-L. Xia, K. Umezawa, T. Kawahara, S. Souma, T. Sato, T. Takahashi, T. Qian, Y. B. Huang, N. Xu, Y. B. Shi, H. Ding, and S.-C. Wang, Phys. Rev. B **84**, 064519 (2011).
[30] S. Thirupathaiah, D. V. Evtushinsky, J. Maletz, V. B. Zabolotnyy, A. A. Kordyuk, T. K. Kim, S. Wurmehl, M. Roslova, I. Morozov, B. Büchner, and S. V. Borisenko, Phys. Rev. B **86**, 214508 (2012).
[31] R. Yu, J-X. Zhu, and Q. Si, arXiv:1306.4184.
[32] C. L. Zhang *et al.*, Phys. Rev. B **88**, 064504 (2013).
[33] G. T. Tan, P. Zheng, X. C. Wang, Y. C. Chen, X. T. Zhang, J. L. Luo, T. Netherton, Y. Song, P. C. Dai, C. L. Zhang, and S. L. Li, Phys. Rev. B **87**, 144512 (2013).
[34] S. W. Oh, A. M. Mounce, J. A. Lee, W. P. Halperin, C. L. Zhang, S. Carr, P. C. Dai, A. P. Reyes, and P. L. Kuhn, Phys. Rev. B **88**, 134518 (2013).
[35] D. K. Pratt, W. Tian, A. Kreyssig, J. L. Zarestky, S. Nandi, N. Ni, S. L. Budko, P. C. Canfield, A. I. Goldman, and R. J. McQueeney, Phys. Rev. Lett. **103**, 087001 (2009).
[36] A. D. Christianson, M. D. Lumsden, S. E. Nagler, G. J. MacDougall, M. A. McGuire, A. S. Sefat, R. Jin, B. C. Sales, and D. Mandrus, Phys. Rev. Lett. **103**, 087002 (2009).
[37] R. Yu and Q. Si, Phys. Rev. B **84**, 235115 (2011); **86**, 085104 (2012).
[38] Z. P. Yin, K. Haule, and G. Kotliar, Nat. Mater. **10**, 932 (2011).
[39] R. Yu and Q. Si, Phys. Rev. Lett. **110**, 146402 (2013).
[40] R. Yu, P. Goswami, Q. Si, P. Nikolic, and J.-X. Zhu, arXiv:1103.3259 [Nat. Commun. (to be published)].
[41] S. Graser, A. F. Kemper, T. A. Maier, H.-P. Cheng, P. J. Hirschfeld, and D. J. Scalapino, Phys. Rev. B **81**, 214503 (2010).
[42] T. Das and A. V. Balatsky, Phys. Rev. Lett. **106**, 157004 (2011).
[43] S. Pailhès, Y. Sidis, P. Bourges, V. Hinkov, A. Ivanov, C. Ulrich, L. P. Regnault, and B. Keimer, Phys. Rev. Lett. **93**, 167001 (2004).